



Forest liming in the face of climate change: the implications of restorative liming on soil organic

2 carbon in mature German forests

Oliver van Straaten¹, Larissa Kulp¹, Guntars O. Martinson², Dan Paul Zederer^{1,3}, Ulrike Talkner^{1*}

4 1. Northwest German Forest Research Institute, Grätzelstr. 2, D-37079 Göttingen, Germany

2. Soil Science of Tropical and Subtropical Ecosystems, University of Göttingen, D-37077
6 Göttingen, Germany

3. Saxon State Office for Environment, Agriculture and Geology, Department of Agriculture,
8 Waldheimer Str. 219, D-01683 Nossen, Germany

* Correspondence email: ulrike.talkner@nw-fva.de



10 Abstract

12 Forest liming is a management tool that has and continues to be used extensively across northern
14 Europe to counteract acidification processes from anthropogenic sulfur and nitrogen (N) deposition.
16 In this study, we quantified how liming affects soil organic carbon (SOC) stocks and attempt to
18 disentangle the mechanisms responsible for the often-contrasting processes that regulate net soil
carbon (C) fluxes. Using a paired-plot experimental design we compared SOC stocks in limed plots with
adjacent unlimed control plots at 28 experimental sites to 60-cm soil depth in mature broadleaf and
coniferous forests across Germany. Historical soil data from a subset of the paired experiment plots
was analyzed to assess how SOC stocks in both control and limed plots had changed between 1990
and 2019.

20 Overall, we found that forest floor C stocks have been accumulating over time, particularly in the
control plots. Liming however largely offsets this organic layer buildup, which means that nutrients
22 remain mobile and are not bound in soil organic matter complexes. Results from the paired plot
analysis showed that forest floor C stocks were significantly lower in limed plots than the control
24 (-34 %, $-8.4 \pm 1.7 \text{ Mg C ha}^{-1}$), but did not significantly affect SOC stocks in the mineral soil, when all sites
are pooled together. In the forest floor layers, SOC stocks exhibited an exponential decrease with
26 increasing pH, highlighting how lime-induced improvements in the biochemical environment stimulate
organic matter (OM) decomposition. Nevertheless, for both forest floor and mineral soils, the
28 magnitude and direction of the belowground C changes hinged directly on the inherent site
characteristics, namely, forest type (conifer versus broadleaf), soil pH, soil texture and the soil SOC
stocks. On the other hand, SOC stock decreases were often offset by other processes that fostered C
30 accumulation, such as improved forest productivity or increased carbon stabilization, which
32 correspondingly translated to an overall variable response by SOC stocks, particularly in the mineral
soil.

34 Lastly, we measured soil carbon dioxide (CO_2) and soil methane (CH_4) flux immediately after a re-liming
event at three of the experimental sites. Here, we found that (1) liming doubles CH_4 uptake in the long-
36 term, (2) highlighted that soil organic matter mineralization processes respond quickly to liming,
though the duration and size of the CO_2 flush varied between sites, and (3) lime-derived CO_2
38 contributed very little to total CO_2 emissions over the measurement period.



1. Introduction

Millions of hectares of forest have been limed in Germany and across northern Europe over the last few decades to counteract soil acidification processes derived from anthropogenic sulfur (S) and nitrogen (N) deposition. Soil acidification is responsible for hindering organic matter decomposition processes and concomitantly immobilizing nutrients and carbon (Shen et al., 2021). The application of lime on acidic soils, as either calcium carbonate (CaCO_3) or dolomite ($\text{CaMg}(\text{CO}_3)_2$) elicits a strong biochemical response by lowering soil acidity, reducing both aluminum (Al) and manganese toxicity and increasing the soil's buffering capacity. These changes subsequently drive a cascade of ecosystem responses, with implications on soil fertility, forest productivity, stand vitality and litter decomposition (Derome et al., 2000; Kreutzer, 1995), which in turn correspondingly affect the ecosystem carbon (C) balance (Melvin et al., 2013; Persson et al., 2021) and soil greenhouse gas (GHG) budgets. The direction and magnitude of ecosystem responses to liming depends on numerous factors, including: (1) the inherent soil characteristics of the site (soil acidity, soil texture, the chemical make-up of the forest floor layer), (2) vegetation characteristics (species distributions, tree density, and stand age), the (3) lime application (type and quantity of lime, and frequency of liming) and (4) ongoing acidification from recent N and S deposition. In this context, both above- and below-ground carbon stocks have been shown to have quite variable responses to liming (Court et al., 2018; Lundström et al., 2003; Melvin et al., 2013; Persson and Ahlström, 1990; Persson et al., 2021).

While, it is broadly reported that liming stimulates soil microbial activity leading to accelerated soil organic matter (SOM) decomposition (Andersson and Nilsson, 2001; Kreutzer, 1995), some studies report either no change in litter and forest floor decomposition (Smolander et al., 1996) or even forest floor accumulations (Derome et al., 2000; Melvin et al., 2013). Soil organic carbon (SOC) stock gains as a result of liming can be attributed to different drivers. First, earthworm abundance is known to increase after liming (Persson et al., 2021) which, by actively incorporating and binding SOM with the mineral soil improves physical properties, such as soil structure and aggregate stability (Bronick and Lal, 2005). Second, physicochemical properties are also affected. Liming induced changes in nutrient-stoichiometry may enhance cation mediated cross-linking between SOM compounds and divalent calcium (Ca) or magnesium (Mg) ions (Kalbitz et al., 2000). It has also been shown that higher soil Ca availability has been shown to increase lignin contents in leaf litter which makes litter more recalcitrant and resistant to decomposition (Eklund and Eliasson, 1990; Xing et al., 2021). Third, liming may introduce nutrient imbalances (such as phosphorus) on decomposer communities and trees (Melvin et al., 2013) that may decrease microbial breakdown of SOM. In addition, liming may induce shifts in microbial community structures, and decrease microbial abundance (Melvin et al., 2013). Lastly, liming-induced improvements in nutrient availability (Jansone et al., 2020; Long et al., 2015), may



74 increase ecosystem productivity which correspondingly can increase SOM inputs from aboveground
(e.g. leaf litter (Lin et al., 2015)) and belowground sources (e.g. root detritus).

76 In this study, we quantified the magnitude of SOC stock changes resulting from forest liming activities,
with the explicit intent to better understand the implications of liming on forest soil greenhouse gas
78 (GHG) budgets. Given the lack of a consistent direction in which SOC stocks respond to liming as
reported in literature, we attempted to disentangle the mechanisms responsible for the often-
80 contrasting processes that regulate net carbon fluxes in the soil. Lastly, we assessed liming effects
across different time scales, ranging from the immediate effects liming has on soil carbon dioxide (CO₂)
82 production, to methane (CH₄) uptake, to long-term changes in soil carbon stocks measured several
decades after liming. The study was implemented at experimental sites in managed mature forests
84 across Germany using both space-for-time substitution and chronosequence approaches.

We hypothesized that liming-induced changes in SOC stocks will be most pronounced at the soil
86 surface. More specifically, we expect that there will be significant decreases in the forest floor layer C
stock because SOM decomposition will be stimulated by reduced pH levels. However, these C losses
88 will be offset if not exceeded, by significant gains in SOC stocks in the topsoil because of improved
ecosystem productivity, increased fine root biomass in the upper mineral soil horizons and increased
90 earthworm activity, which will improve soil structure thereby protecting SOM from mineralization.

2. Methods and Materials

92 2.1 Experimental study sites

Liming effects on soil organic carbon stocks were determined at 28 liming experiment sites distributed
94 across Germany (Figure A1). All sites consisted of mature forest stands whereby all, except one (HLI
2680) were managed, meaning sites were occasionally selectively harvested. Lime was applied in
96 different forms (dolomite (CaMg(CO₃)₂) and calcium carbonate (CaCO₃)) and in differing quantities,
ranging from a total between 2-9 tons per hectare spread over multiple application dates (Table 1).
98 The last lime application at most sites was typically 20 to 30 years prior to our sampling, and therefore
findings reflect the long-term effects liming has on belowground carbon. The experiment was
100 conducted using a paired plot design, where each site consisted of a limed plot adjacent to a control
plot which was not limed. In total, for this analysis, we sampled nine sites with European beech (*Fagus
102 sylvatica* L.), two with common oak (*Quercus robur* L.), 16 with Norway spruce (*Picea abies* L. karst.)
and one European red pine (*Pinus sylvestris* L.) site. General site characteristics are described in Table
104 1. At two spruce sites (GOH 155, SEG 244) we only had data from the forest floor layers, and not the
mineral soil as soil bulk density data were unavailable. Nitrogen deposition was ascertained from the
106 German Environment Agency (UBA, 2019).



Table 1: Site characteristics and liming details of the 28 experimental sites. Soil texture measurements were only made at 16 sites.

| Site name | Experiment and liming details | | | | Climate | | | Soil | | | | |
|---|--|-----------------------------|-------------------|--|-----------------------------------|--|---------------------------------|----------------------|---|--|--|--|
| | Plot size (limed/ control) [ha] | Number of times limed | Type of lime † | Lime quantity [Mg ha ⁻¹] | ANC‡ [kmol. ha ⁻¹] | Mean annual precip. [mm a ⁻¹] | Mean annual temp. [°C] | Elevation [m.asl] | Nitrogen deposition [kg N ha ⁻¹ yr ⁻¹] | Soil pH (H ₂ O; 0-5 cm; limed/control) [%] | Soil base saturation (0-5cm; limed/control) [%] | Soil texture (30-60 cm; sand / silt / clay) [%] |
| Beech sites: | | | | | | | | | | | | |
| Beerfelden 767A | 0.25 / 0.1 | 2 | B, B | 1, 1 | 42 | 977 | 8.9 | 447 | 14 | 4.1 / 3.9 | 30 / 7 | 70 / 18 / 12 |
| Dassel 4227 | 0.2 / 0.1435 | 2 | A, B | 5, 3 | 140 | 1221 | 7.7 | 430 | 19 | 4.8 / 3.7 | 30 / 7 | 50 / 36 / 14 |
| Eutin 402 | 0.25 / 0.25 | 2 | B, B | 3, 3 | 109 | 746 | 8.2 | 55 | 22 | 4.9 / 4.1 | 67 / 11 | n.a. |
| Göhrde 157 | 0.25 / 0.25 | 2 | A, B | 5, 3 | 140 | 733 | 8.8 | 100 | 16 | 4.6 / 3.7 | 40 / 11 | 93 / 4 / 3 |
| Grünenplan 142 | 0.25 / 0.25 | 3 | B(G), B, B | 5, 3, 3 | 133 | 920 | 8.9 | 260 | 19 | 5.2 / 4.1 | 52 / 15 | 4 / 73 / 23 |
| Grünenplan 51 | 0.3 / 0.3 | 1 | B(G) | 5 | 75 | 920 | 8.9 | 330 | 19 | 5.7 / 5.0 | 93 / 73 | n.a. |
| Hess. Lichtenau 2680 | 0.3 / 0.3 | 2 | B, B | 1, 1 | 41 | 970 | 7.3 | 487 | 17 | 4.2 / 4.1 | 10 / 7 | 32 / 50 / 18 |
| Josgrund 2268 | 0.3 / 0.3 | 2 | B, B | 1, 1 | 41 | 1050 | 8.5 | 385 | 13 | 4.7 / 4.3 | 49 / 16 | 58 / 30 / 12 |
| Sellhorn 34 | 0.15 / 0.15 | 2 | A, B | 5, 3 | 148 | 849 | 8.9 | 110 | 19 | 4.6 / 4.0 | 56 / 13 | 85 / 11 / 4 |
| Oak sites: | | | | | | | | | | | | |
| Göhrde 140 | 0.25 / 0.25 | 2 | A, B | 5, 3 | 140 | 733 | 8.8 | 95 | 16 | 4.7 / 4.1 | 37 / 7 | n.a. |
| Sellhorn 66 | 0.4 / 0.4 | 2 | A, B | 5, 3 | 140 | 849 | 8.9 | 110 | 20 | 4.4 / 4.2 | 48 / 17 | n.a. |
| Spruce sites: | | | | | | | | | | | | |
| Bad Waldsee | 4.28 / 5.21 | 3 | A, B | 2, 6 | 171 | 970 | 8.6 | 571 | 19 | 5.8 / 3.9 | 91 / 14 | 59 / 28 / 13 |
| Beerfelden 767B | 0.15 / 0.15 | 2 | B, B | 1, 1 | 42 | 977 | 8.9 | 442 | 15 | 3.5 / 3.5 | 8 / 5 | n.a. |
| Dassel 325 | 0.2 / 0.1 | 3 | A, B, B | 5, 3, 3 | 140 | 1221 | 6.9 | 390 | 20 | 4.4 / 3.8 | 46 / 5 | n.a. |
| Ellwangen | 10.24 / 1.32 | 3 | A, B | 3, 6 | 171 | 847 | 8.8 | 482 | 16 | 6.3 / 4.0 | 92 / 24 | 64 / 26 / 10 |
| Freudenstadt | 7.71 / 3.46 | 3 | A, B | 3, 6 | 171 | 1516 | 7.4 | 748 | 13 | 4.6 / 3.7 | 70 / 6 | 75 / 16 / 8 |
| Göhrde 155 * | 0.25 / 0.25 | 2 | A, B | 5, 3 | 140 | 733 | 8.8 | 80 | 18 | - | - | - |
| Heidelberg | 2.13 / 0.82 | 3 | A, B | 3, 6 | 171 | 1193 | 8.8 | 477 | 14 | 6.6 / 3.6 | 98 / 14 | 69 / 22 / 9 |
| Herzogenweiler | 8.28 / 3.28 | 3 | A,, B | 3, 6 | 171 | 1203 | 6.7 | 909 | 12 | 5.9 / 3.8 | 95 / 5 | 55 / 24 / 21 |
| Horb | 8.35 / 2.27 | 3 | A, B | 3, 6 | 171 | 969 | 8.2 | 623 | 12 | 4.7 / 4.1 | 55 / 32 | 44 / 36 / 20 |
| Hospital | 2.59 / 0.51 | 3 | A, B | 3, 6 | 171 | 827 | 8 | 645 | 18 | 5.7 / 3.8 | 91 / 11 | 36 / 45 / 19 |
| Lauterberg 2023 | 0.25 / 0.25 | 3 | D, B, B | 1, 3, 3 | 128 | 1220 | 6.1 | 570 | 22 | 4.9 / 4.1 | 46 / 8 | n.a. |
| Lauterberg 75 | 0.25 / 0.25 | 2 | D, E | 1, 3 | 131 | 1454 | 5.1 | 790 | 25 | 4.4 / 4.3 | 10 / 5 | n.a. |
| Rantau 50 | 0.2217 / 0.25 | 3 | C, B, B | 3, 3, 3 | 140 | 807 | 8.4 | 35 | 26 | 3.9 / 3.6 | 30 / 8 | n.a. |
| Segeberg 244 * | 0.25 / 0.25 | 3 | B, B, B | 3, 3, 3 | 109 | 800 | 8.3 | 34 | 26 | - | - | - |
| Segeberg 517 | 0.25 / 0.25 | 3 | B, B, B | 3, 3, 3 | 109 | 844 | 8.3 | 20 | 26 | 4.1 / 3.7 | 34 / 11 | n.a. |
| Weithard | 1.25 / 0.59 | 3 | A(F), B | 3, 6 | 171 | 832 | 8.1 | 627 | 16 | 5.1 / 3.8 | 80 / 10 | 35 / 47 / 18 |
| Pine sites: | | | | | | | | | | | | |
| Göhrde 129 | 0.25 / 0.25 | 3 | A, B, B | 5, 3, 3 | 140 | 733 | 8.8 | 70 | 18 | 4.8 / 4.1 | 49 / 12 | n.a. |
| Only forest floor layer sampled in this plot; † Types of lime: A = Calcium carbonate, B = Dolomite; C = Marl lime, D = Thomas-phosphate, E = Slag lime, F = Potassium sulfate, G = Rock phosphate; ‡ Acid neutralizing capacity | | | | | | | | | | | | |

* Only forest floor layer sampled in this plot; † Types of lime: A = Calcium carbonate, B = Dolomite; C = Marl lime, D = Thomas-phosphate, E = Slag lime, F = Potassium sulfate; ‡ Acid neutralizing capacity



2.2 Soil organic carbon stocks

We collected soil and forest floor samples from both limed and control plots from each site at four locations distributed around the plot. Samples were taken from the forest floor (L/O_r and O_h) as well as from the mineral soil at predefined depths (0-5, 5-10, 10-30 and 30-60 cm). Samples of the forest floor and the topsoil (0-30 cm) were taken using a root auger (diameter 8 cm) and samples of the subsoil (30-60 cm) using a gouge auger (diameter 3 cm). At each of the four sampling locations per plot, three samples were taken for each depth and pooled. Forest floor samples were subsequently oven dried at 60 °C, sieved (2 mm) and ground, mineral soil samples were oven dried at 40 °C, sieved (2 mm) and ground. Both forest floor and mineral soil samples were then analyzed for carbon (C) and nitrogen (N) contents using a CN analyzer (Euro EA - CN Elemental Analyzer, HEKAtech GmbH, Wegberg, Germany). Sieved forest floor and mineral soil samples were also analyzed for pH in a 1:2.5 H₂O solution and mineral soil samples for exchangeable cations (Ca, Mg, K, Na, Al, Fe, Mn) using an ICP-AES instrument (Thermo Scientific iCAP 7400 Radial, Thermo Scientific, Dreieich, Germany). Base saturation was calculated as percentage exchangeable base cations of the effective cation exchange capacity (ECEC). Soil texture was determined using the pipette method at 16 experiment sites.

Soil bulk density and the mineral soil dry mass per unit area was determined using a modified version of the Blake and Hartge (1986) core method. Samples were taken at four soil pits per plot for the same respective depths where samples were taken for chemical analysis. Depending on the size and relative abundance of stones observed in the soil profile, different approaches were employed to estimate the bulk density of the soil fine-fraction. Methods and equations are described by König et al. (2014). All samples were oven dried at 105 °C for 48 hours and subsequently weighed. Volumes of coarse fragments were determined using the volume displacement method. For the mineral soil, we calculated the fine earth soil mass per unit area for each respective sampling layer as follows:

$$\text{Fine earth mass per unit area} = \text{BD} * (1 - \text{stone content}) * d * 10 \quad (1)$$

Where, fine earth soil mass per unit area is in kg m⁻², BD is the soil bulk density in g cm⁻³, stone content is relative volumetric coarse fragment content, d is the thickness (depth) of the sampling horizon in centimeters and 10 is a conversion factor for converting g cm⁻² to kg m⁻².

The organic layer dry mass per unit area was determined at the same four sampling locations where the samples for the chemical analysis were collected using a root auger (diameter 8 cm). The organic material from within the auger was collected and separated into the two forest floor layers (L/O_r and O_h). Roots and plant debris larger than 2 cm in size were removed from the sample, whereupon samples were oven dried and weighed (König et al., 2014):

$$\text{Organic layer dry mass per unit area} = (\text{MH} * 100) / \text{SA} * 10 \quad (2)$$



whereby, organic layer mass per unit area is in kg m^{-2} , MH is the dry mass of the organic layer in grams, and SA is the surface area that was sampled in cm^2 , and 10 is a conversion factor for converting to kg m^{-2} . Mineral and forest floor organic carbon stocks were calculated as follows:

$$\text{SOC stock} = \frac{\text{OC} * \text{MuA}}{100} \quad (3)$$

whereby, SOC stock is in Mg C ha^{-1} , OC is the organic C content in g kg^{-1} , MuA is the mass per unit area in kg m^{-2} , and 100 is a conversion factor for converting to Mg C ha^{-1} .

SOC stocks in the limed plots were corrected for fixed-depth differences incurred because of liming-induced changes in soil bulk density (Figure A2) by using the equivalent soil mass (ESM) approach described by Wendt and Hauser (2013). This approach fits a cubic spline curve of cumulative organic carbon stocks with the corresponding soil mass of the reference profile.

Effects of liming were evaluated using two approaches. First, the difference in soil C stocks between limed and control plots were calculated to assess the relative differences. Second, a chronosequence approach was used to assess temporal changes in soil C stocks using historic data, between 1990 and 2019, collected at a subset of the paired experiment sites (forest floor: $n = 17$, mineral soil: $n = 13$). Table A1 (in the Supplement) shows the years when forest floor and mineral soil samples were collected. The change in SOC stocks over time was estimated by calculating the slope of a linear best fit function of the SOC stock values over time. In this analysis, we assumed that soil density did not change during this time and accordingly we used bulk density estimates from the most recent measurement date.

2.3 Short term effects of liming on soil CO_2 and CH_4 fluxes

Soil carbon dioxide (CO_2) and methane (CH_4) fluxes were measured at three beech forest sites (Dassel 4227 (DAS 4227), Sellhorn 34 (SEL 34), Göhrde 157 (GOH 157) to assess both short and long-term effects of liming. All three sites were freshly re-limed with an equivalent of $3 \text{ Mg CaCO}_3 \text{ ha}^{-1}$ in August-September 2020. Accordingly, the measurements made after these liming events reflect the short-term effects of liming on soil respiration and soil methane fluxes. The soil trace gas fluxes were measured using the vented static chamber method. Round chamber bases (polyvinyl chloride, covering a ground area of 0.07 m^2) were inserted 1–2 cm into the soil surface at four randomly locations within each plot. These chamber bases were covered with polyethylene lid ($\sim 22 \text{ L}$ headspace volume), from which gas samples were collected at 20-min intervals for one hour (2, 22, 42 and 62 min) and stored in pre-evacuated 12 mL Labco Exetainers® (Labco Limited, Lampeter, UK). To minimize effects from diurnal fluctuations we randomized the order the plots were measured during each measurement campaign. Gas samples were analyzed using a gas chromatograph (GC, SRI 8610c, SRI Instruments,



174 Torrance, USA), equipped with a flame ionization detector to measure CH₄ and CO₂. The latter gas
species was analyzed by converting it to CH₄, using a built-in methanizer in the GC. The GC was
176 calibrated prior to each analysis using three calibration gases (Deuste Steininger GmbH, Mühlhausen,
Germany), spanning the concentration range of the field samples. Soil gas fluxes were calculated using
178 the ideal gas law, based on the linear increase of gas concentrations in the chamber over time and
corrected with air temperature and atmospheric pressure measured at the time of sampling. A
180 positive flux indicates a net emission, while a negative flux indicates a net consumption. In parallel to
the greenhouse gas flux measurements, we also measured air pressure, soil and air temperature and
182 chamber volume during each measurement.

In early September 2020, we measured soil CO₂ and CH₄ fluxes at one site (DAS 4227) three times in
184 the week prior to lime application (on Sep 7, 2020) so as to evaluate baseline fluxes and to determine
whether there were long-term effects of previous liming events still evident. After liming, we measured
186 GHG fluxes weekly for two months (to Nov. 3, 2020) to evaluate immediate effects of the liming.
Subsequently, in the spring of 2021, we resumed gas flux measurements on a bi-weekly basis at the
188 DAS 4227 site, and additionally also commenced measurements at the two other sites (SEL 34, GOH
157). These measurements were made from Mar. 11, 2021 to Jul. 8, 2021.

190 **2.4 Calculation of lime-derived CO₂ emissions**

The proportion of lime-derived CO₂ to the overall CO₂ flux, was determined using δ¹³C stable isotope
192 approaches and a two-pool mixing model. The ¹³C signature of newly formed CO₂ (δ_n) between time
point t = 1 (δ₁) and t = 2 (δ₂), and the newly formed CO₂ fraction at t = 2 is given by the following mass
194 balance equation (Martinson et al., 2018):

$$\delta_2 = f_n \delta_n + (1 - f_n) \delta_1 \quad (4)$$

196 The fraction of lime-derived CO₂ to total CO₂ emissions is calculated following the two-pool mixing
model under the assumption that (1) biologically-derived ¹³CO₂ is equal between limed and unlimed
198 plots and (2) CO₂ from lime carbonates and from lime-induced respiration is in isotopic equilibrium:

$$f = \frac{(\delta + \delta_0)}{(\delta_1 + \delta_0)} \quad (5)$$

200 whereby, δ is the isotopic signature of ¹³CO₂ from limed plots, δ₀ the isotopic signatures of ¹³CO₂ from
unlimed plots, δ₁ the isotopic signature of lime.

202 Carbon isotope signatures (δ¹³C) were determined by isotope ratio mass spectrometry at the Centre
for Stable Isotope Research and Analysis (KOSI) at the University of Göttingen, Germany.

204



206 **2.5 Statistical analysis**

Liming effects on SOC stocks at each soil depth were tested using linear mixed effects (LME) models
 208 (Crawley, 2013). In these models, the C stock was the response variable, the treatment (control, limed)
 was the fixed effect, and the site was the random effect. For the soil trace gas flux measurements, the
 210 treatment was considered a fixed effect and the measurement date were considered random effects.
 Significance levels were tested separately for each site. Differences were considered significant if
 212 $P \leq 0.05$ and marginally significant if $P \leq 0.1$. The input C stock data as well as the output model
 residuals were tested for normality using Shapiro–Wilk test. To gain an insight into the underlying
 214 factors regulating C stocks in the control (unamended plots) and the relative changes in C stocks as a
 result of liming, we used Spearman’s rank correlation analyses to assess how C stocks correlated with
 216 climatic parameters, stand parameter as well as the inherent soil properties (of the control plot) and
 the liming induced changes in soil properties (difference between limed and control plots). The
 218 goodness of fit of the non-linear best-fit models were assessed using Pearson correlation analyses
 between model-predicted values and measured values. All statistical analyses were carried out using
 220 R, version 4.0.02 (R Core Team, 2020).

222 **3. Results**

3.1 SOC stocks in the control plots: magnitude and drivers

224 There was a large variability in SOC stocks across the experimental sites, ranging between 49 and 366
 Mg C ha⁻¹ (forest floor to 60 cm, in the control plots). In the soil profile, SOC content was highest in the
 226 forest floor layer and decreased with soil depth (Figure A3a). In the control plots, 23 % of the total SOC
 stock was found in the forest floor layer, 27 % in the topsoil (0-10 cm), and the remaining 50 % was
 228 found below 10 cm depth (10-60 cm) (Figure A3b). Coniferous forests stored approximately 38 % more
 carbon than broadleaf forests (conifer: 157 ± 17 Mg C ha⁻¹ (mean \pm standard error (SE)), broadleaf:
 230 97 ± 9 Mg C ha⁻¹), where differences were most pronounced in the forest floor L/O_f horizon and below
 10 cm soil depth. Soil bulk density was lowest at the soil surface (0-5 cm) and increased with soil depth
 232 (Figure A2a). SOC stocks in the mineral soil correlated significantly with soil chemical and physical
 properties, but not with climatic variables such as temperature, precipitation, or elevation (Table A2).
 234 In the forest floor layers, SOC stocks were correlated with both N deposition and pH. For the latter,
 there was an exponential decrease in the SOC stocks with increasing pH (Figure 1), where, particularly
 236 in the L/O_f layer, there was large decline in SOC stocks when pH increased from 3.5 to 4.5. Next, N-
 deposition exhibited a significant positive correlation with SOC stock in the L/O_f horizon, whereby



these effects were only evident in coniferous forests (Figure A4a). This trend was largely driven by the strong linear correlation present between C content and N deposition (Figure A4b), and although the mass of the L/O_f horizon correspondingly increased with N deposition, the most increases were only consistent when N deposition was higher than 25 kg N ha⁻¹ yr⁻¹ (n = 4) (Figure A4c).

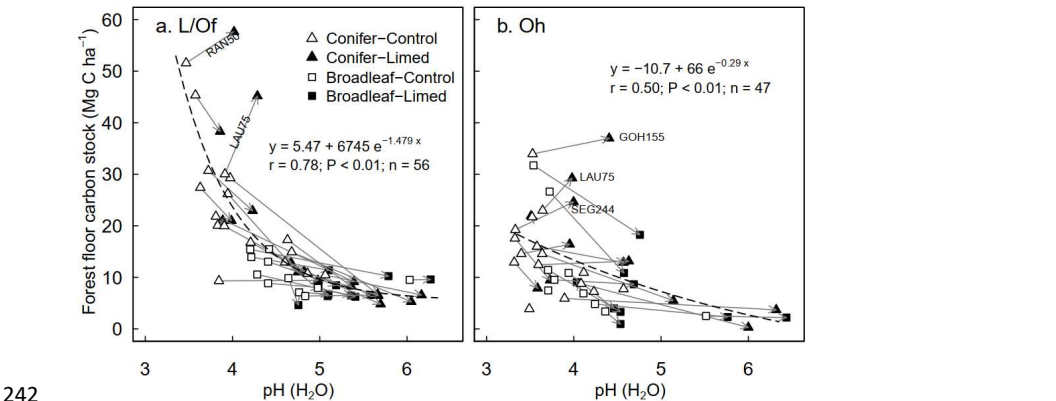


Figure 1: Relationship between the pH of the forest floor layer and the carbon stock of the (a) L/O_f and (b) O_h horizons. The arrows indicate the change from control to limed plots. Missing arrows (in b.) are because the O_h horizon disappeared at those sites as a result of liming. The r is the Pearson correlation coefficients between observed and fitted values. RAN50 is Rantza 50, LAU75 is Lauterberg 75, GOH155 is the Göhrde 155, SEG 244 is the Segeberg 244 site.

In the mineral soil, SOC stocks correlated with soil texture fractions. This was evident in the significant negative correlations between SOC stock and sand contents at 0-5 cm and 5-10 cm, as well as the positive correlation with clay content at 10-30 cm (Table A2). In the subsoil (30-60 cm), SOC stocks exhibited a similar exponential decay relationship with soil pH as the forest floor layers (data not shown).

3.2 SOC stock response to liming: chronosequence approach

At a subset of experimental sites where historical data were available, forest floor C stocks in the control plots increased in time (0.5 ± 0.1 Mg C ha⁻¹ yr⁻¹; Figure 2a), whereby the increases were largely driven by C accumulations at coniferous forest site (0.8 ± 0.3 Mg C ha⁻¹ yr⁻¹). Although forest floor SOC stocks in the limed plots also increased over time, the accumulation rates in the L/O_f horizon were significantly lower than the control (Figure 2b). In the mineral soil, there were no significant changes in SOC stocks at any depth during this period. Nevertheless, when C stock change rates were compared between limed and control plots, liming did bolster C accumulation rates slightly at 5-10 cm depth.

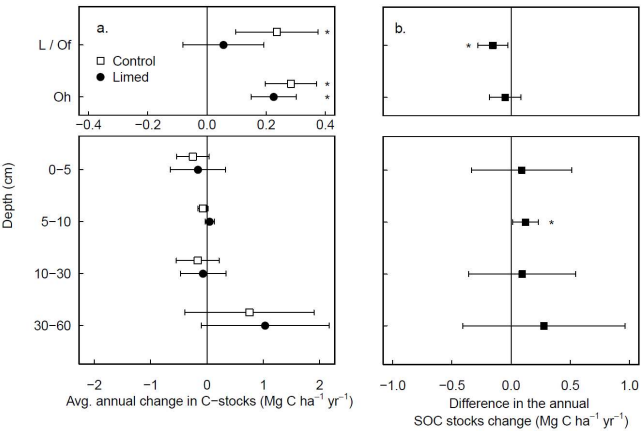


Figure 2: Average (\pm 95 % T-test-confidence interval) annual changes in SOC stocks experienced over the last two decades in a) both the control and limed plots and b) the difference between the limed and control plots. Statistical significance was tested using LME models for each respective soil depth / layer at $P \leq 0.05$ (*).

3.3 SOC stock response to liming: paired plot approach

Total SOC stocks (forest floor to 60 cm) were comparable between the limed (126 ± 12 Mg C ha⁻¹) and control plots (132 ± 12 Mg C ha⁻¹) (Figure A3b). In the forest floor layer, liming significantly reduced SOC stocks by 34 ± 12 % (equivalent to 8.4 ± 3.6 Mg C ha⁻¹, Figure 3a), which reflects reductions in both C content (-8.8 ± 2.4 %) as well as the forest floor dry mass (-26.1 ± 6.7 %). Both broadleaf and coniferous forests had similar SOC losses in the forest floor layer both in magnitude (broadleaf: -8.1 ± 4.8 Mg C ha⁻¹, coniferous: -8.6 ± 2.7 Mg C ha⁻¹) and in overall proportion of the forest floor SOC stock (Figure 3b).

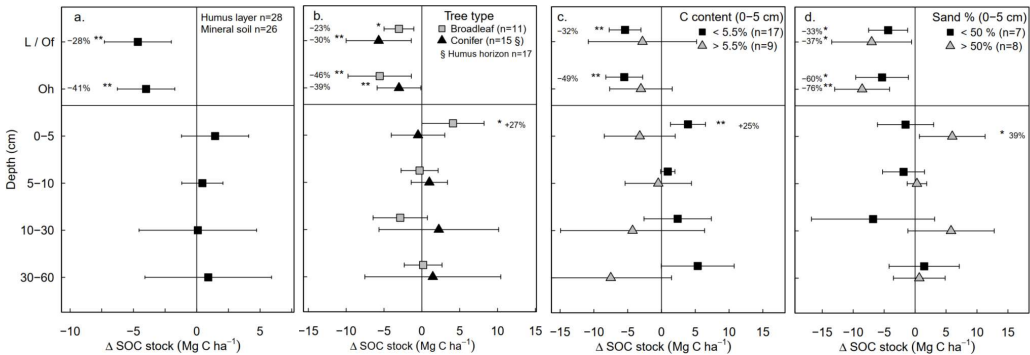
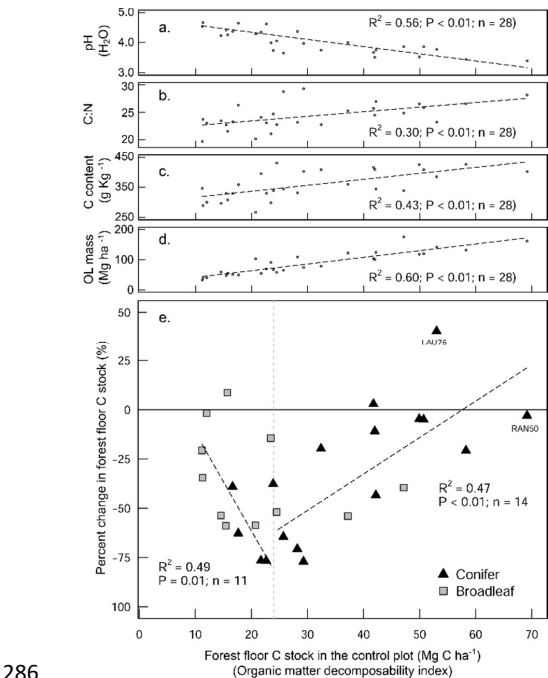


Figure 3: Changes in mean soil organic carbon stock (limed - control) as a result of liming (a) for all plots in the experiment, and classified by (b) tree types and (c) inherent C content of the control plots and (d) site sand percent from 0-5 cm depth. Error bars indicate the 95 % confidence intervals based on Student's T distribution. Statistical significance was tested using LME models for each respective soil depth / layer and grouping at $P \leq 0.05$ (*), and $P \leq 0.01$ (**).



280 The liming quantities which are responsible for the changes in soil pH, exhibited a negative linear
relationship with SOC stock changes (Figure A5), indicating that higher liming dosages result in larger
282 SOC losses. In the forest floor layer, the proportion of C losses or C gains (at a few sites) could further
be explained by the initial C stock present on the site (control plot C stock), whereby the C losses were
284 largest at sites with medium amounts of stored C (between 20 and 35 Mg C ha⁻¹), and less pronounced
(or even positive) at sites with either little or large C stocks present in the reference state (Figure 4e).

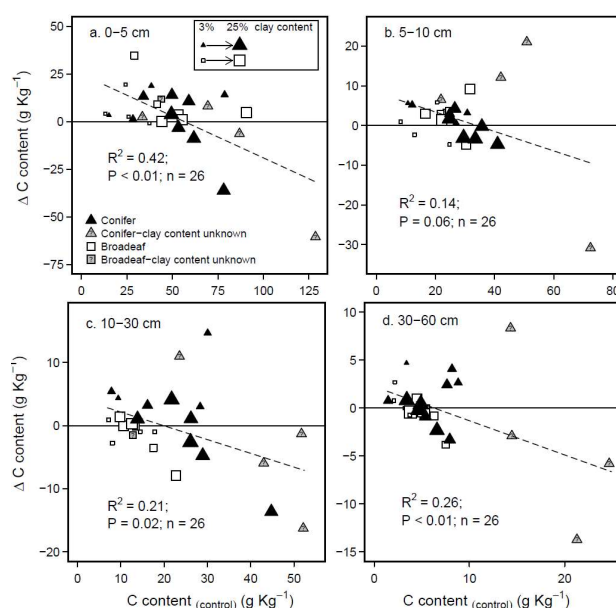


286 **Figure 4:** Scatterplot diagrams showing how the forest floor SOC stocks in the control plots relate to a)
288 pH (H₂O), b) the C:N ratio, c) the C content of the forest floor layer and d) the forest floor (organic layer
290 (OL)) biomass. These four parameters show how the forest floor C stock in the control plots is a good
292 index of organic matter decomposability. The scatterplot in e) shows the percentage change in the
forest floor C stock as a result of liming in relation to the forest floor decomposability index (forest
294 floor C stocks of the control plots). The two linear regression lines in e) show C change for the different
forest floor stock ranges (above and below 25 Mg C ha⁻¹). LAU75 is Lauterberg 75 and RAN50 is Rantza
50.

296 Overall, there were no significant changes in mineral SOC stock at any depth (Figure 3a), when all sites
are pooled together. Unlike coniferous forests, broadleaf forest plots (n = 11) exhibited significant
298 increases in SOC stock in the topsoil (0-5 cm) (3.5 ± 1.9 Mg C ha⁻¹, Figure 3b). While it was not significant
for SOC stock changes (Table A3), changes in soil C content hinged on the inherent (control) C content
300 (Figure 5). In the mineral soil, the experimental sites that initially had low C contents exhibited
increases in C, while sites with already high C contents exhibited decreases. Accordingly, when sites



302 were classified as having either inherently high C contents ($>5.5\%$ at 0–5 cm, $n = 9$) or inherently low
C contents ($<5.5\%$ at 0–5 cm, $n = 17$), large differences in SOC stocks between the two categories
304 became evident in soil profile (Figure 3c). Namely, SOC stocks increased significantly at sites which
inherently had low C contents in the control plots (C content $<5.5\%$ at 0–5 cm, Figure 3c). Here, gains
306 in mineral SOC stocks (0–60 cm) were significantly higher than zero ($13.1 \pm 4.7 \text{ Mg C ha}^{-1}$), although
these gains were offset by the SOC losses in the forest floor layers ($-10.6 \pm 5.6 \text{ Mg C ha}^{-1}$). Conversely,
308 the sites that inherently had high SOC contents in the control plots (C content $>5.5\%$ at 0–5 cm), did
not exhibit significant changes in SOC stock at any soil depth throughout the profile, whereby there
310 was a tendency to have SOC losses throughout the profile (forest floor: $-5.6 \pm 3.5 \text{ Mg C ha}^{-1}$, mineral
soil 0–60 cm: $-16.4 \pm 3.8 \text{ Mg C ha}^{-1}$). Next, SOC stocks significantly increased in the 0–5 cm layer in sandy
312 sites ($<50\%$ sand, Figure 3d), while sites with higher clay and silt fractions exhibited no change in SOC
stocks at any depth. In both the forest floor O_h horizon and at 0–5 cm depth, soil C:N ratios decreased
314 significantly as a result of liming (Figure A6a).



316

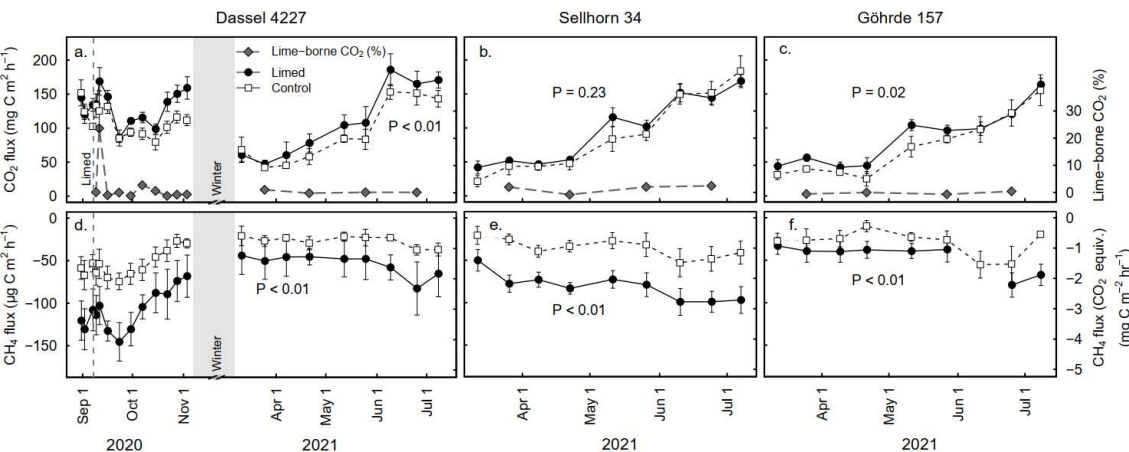
Figure 5: Scatterplot diagrams showing SOC contents in the control plots in relation to the liming induced changes in SOC contents for the different sampling depths in the soil profile. The size of the symbol reflects the amount of clay present at each site. Grey points indicate sites where soil texture was not known.

3.4 Liming effects on soil CO₂ and CH₄ fluxes in beech forests

322 The soil greenhouse gas flux measurements made prior to re-liming at the DAS 4227 site (indicative of the long-term effects of liming) showed that (1) there were no significant differences in soil respiration



324 rates between limed and control plots ($P = 0.49$, Figure 6a), but that (2) methane uptake was twice as
high in the limed plots compared to the control ($P < 0.01$, Figure 6d-f). Immediately following the re-
326 liming, soil CO_2 fluxes increased and remained consistently higher than the control ($P < 0.01$, Figure 6a)
for the duration of the measurements. Soil methane uptake on the other hand did not respond to the
328 liming application, and remained consistently lower than the control ($P < 0.01$ Figure 6d).



330 **Figure 6:** Mean (\pm SE) soil CO_2 (a-c) and CH_4 fluxes (d-f) at the Dassel 4227, Sellhorn 34 and Göhrde 157
332 sites in limed and control plots. The grey line in (a-c) indicate the percentage of lime- derived CO_2 of
the total CO_2 flux. P-values indicate the significance level between treatments based on LME models.
334 At the Dassel 4227 site, the three baseline measurements made prior to re-liming give an indication of
existing long-term differences in soil CO_2 and soil CH_4 fluxes. At time there were no significant
treatment differences for CO_2 fluxes ($P = 0.49$) but CH_4 fluxes were significant between the treatments
336 ($P < 0.01$). At each site $3 \text{ Mg CaCO}_3 \text{ ha}^{-1}$ were applied in the late summer of 2020. Soil CH_4 fluxes are
presented in both actual measured units and CO_2 equivalence, based on a global warming potential of
338 28.

340 Soil respiration measurements made at the beginning of the growing season of 2021 (6 to 10 months
after liming) at the three sites (GOH 157, DAS 4227, SEL 34) show that overall soil CO_2 fluxes were
342 significantly higher ($23 \pm 7\%$, $P < 0.01$) in the limed plots in comparison to the control (Figure 6a-c).
The strength of the liming response however depended on the site, where both GOH 157 and
344 DAS 4227 exhibited significant increases in CO_2 fluxes, while the SEL 34 site did not show any significant
change in CO_2 flux (Figure 6b). Overall, soil methane uptake was significantly higher in the limed
346 treatments ($P < 0.01$) and was on average two times higher than the control at all three sites (Figure
6d-f).

348 Using a stable isotope analysis approach, the overall contribution of lime- derived CO_2 was low,
averaging 2.7% of the total CO_2 flux in the first two months after lime application at the DAS 4227 site.
350 At this site, there was only one short-lived lime-derived CO_2 pulse immediately after a rewetting event



five days after liming (Figure 6a) which accounted for 23 % of total (biotic and abiotic) CO₂ emissions.

The lime- derived CO₂ contribution remained negligible the following spring when we measured at the three sites, averaging 0.7 ± 0.5 % (n = 3) of the total CO₂ flux.

4. Discussion

4.1 Liming effects on organic C stocks in the forest floor layers

Over the last three decades, forest floor C stocks have gradually been accumulating in both the limed and control plots (Figure 2a), with increases most being pronounced at coniferous sites. These gains likely reflect the influence of elevated N depositions (among other factors) that can (1) enhanced tree growth accordingly increase litter inputs (Court et al., 2018, Van der Perre et al., 2012) and/or (2) constrain organic matter decomposition rates (Knorr et al., 2005). The effects of N additions were particularly evident at our coniferous forest plots where sites with higher N deposition had larger forest floor carbon accumulations (Figure A4).

Considering the biochemical environment plays an intrinsic role in many soil biological processes (Andersson and Nilsson, 2001; Persson et al., 2021; Melvin et al., 2013), changes in soil pH from liming can and will cause a cascade of responses that concomitantly affect the net soil C balance. In the temporal (chronosequence) analysis, the small absolute gains in the forest floor C stocks measured in the limed plots over time (Figure 2a) were significantly lower than those measured in the unlimed control plots (Figure 2b), highlighting how lime applications have (in the majority of sites) promoted organic matter mineralization and offset forest floor OM accumulations. Since overall C stock gains were comparatively minor (in relation to the control), it indicates that lime applications here helped maintain stable organic matter decomposition and nutrient cycling rates. These results are further substantiated in the paired approach analysis, where a larger number of plots were included (Figure 3a). Although this analysis partly contrast the findings reported by the German National Forest Soil Inventory (which showed that liming decreased forest floor C stocks while unlimed plots remained unchanged over time (Grüneberg et al., 2019)), both of these studies show the same relative trends: namely that liming stimulates organic matter mineralization. This too is corroborated by most other studies (Court et al., 2018; Kreutzer, 1995; Marschner and Wilczynski, 1991; Persson et al., 2021), whereby some publications (Derome et al., 2000; Melvin et al., 2013) have reported the opposite, namely that under certain conditions liming can actually increase soil C stocks.

In this study, we found a clear exponential relationship evident between forest floor C stocks and forest floor layer pH (Figure 1) namely poor sites with acidic pH had high C accumulations in contrast to sites with higher pH that had lower C stocks. In conjunction with increased microbial-induced SOM



384 mineralization, it is also likely that increases in earthworm activity, which is known to increase with
liming (Persson et al., 2021), will have assisted the breakup of the litter and the mixing of the organic
386 matter with soil particles and microorganisms throughout the soil layer (Kreutzer, 1995, Persson et al.,
2021). Next, the improvements in forest floor composition and morphology were also visually evident
388 at six of the 28 experimental sites, where the humus-form classification improved along the moder to
mull gradient. Moreover, there was also an additive effect of the lime quantity on C stock losses, where
390 higher lime applications translated to larger C differences with the limed plots (Siepel et al., 2019,
Figure A5). This is not surprising, considering that the more lime applied, the stronger was the
392 corresponding effect on soil pH (for example, the change in pH in response to the lime's acid
neutralizing capacity at 0-5 cm was highly significant ($R^2 = 0.43$, $P < 0.01$)).

394 The proportional net change in forest floor C stocks, either C losses or C gains (in relation to the control)
which were observed at a few plots, could best be explained when put in the context of the C stock
396 present in the control plot. This is because the inherent forest floor C stock (in the control plots) is a
good index of organic matter decomposability (hereafter called the decomposability index) showing
398 the integral effect of different biochemical drivers (such as pH and litter quality) that regulate SOM
breakdown. For instance, sites with high C stocks had correspondingly acidic pHs (Figure 4a), high C:N
400 ratios (Figure 4b), and both high C contents (Figure 4c) and high SOM mass (Figure 4d). This contrasts
those sites with inherently low forest floor C stocks which had higher pH, low C:N ratios, low C contents
402 and thin organic matter layers. When we use the C stock of the control plots as an index of carbon
bioaccumulation, we see that liming effects on forest floor C stocks are most pronounced at sites with
404 intermediate amounts of carbon ($18\text{--}35 \text{ Mg C ha}^{-1}$), and less prominent at the other ends of the index
(Figure 4e). First, liming additions to sites which had inherently low forest floor C stocks (characterized
406 by thin SOM layers and high pH) exhibited only small proportional losses in overall C stocks (Figure 4e).
This minor response is because these sites already had relatively high pH values and the addition of
408 lime did not change the biogeochemical environment dramatically, and accordingly there were no
large changes in forest floor C stocks. Next, further along this decomposability index, sites with
410 intermediate amounts of carbon exhibited large C losses (up to 75 % decreases). This is because the
application of lime improved the biochemical environment for microbial communities thereby
412 stimulating organic matter decomposition, which led to strong C losses at these sites. Finally, further
along this decomposability index, at sites having inherently high forest floor C stocks the application
414 of lime had an increasingly muted effect on C losses, ultimately leading to C gains at some sites (for
example LAU75). Sites at this end of the spectrum were particular poor, having inherently low pH and
416 thick organic horizons. Here we suspect that more lime had to be applied in order to buffer soil
acidification in an extent that leads to pH improvements favorable for soil microorganisms and other
418 soil biota. Thus, microbial activity and accordingly also decomposition rates remained more or less



unchanged. We suspect that the inherent biochemical conditions at this end of the spectrum are likely similar to those reported by Melvin et al. (2013) in hardwood forests in the USA and by Derome et al. (1990, 2000) in spruce and pine stands in Finland, who both report significant gains in SOC stocks as a result of liming.

4.2 Liming effects on organic carbon stocks in the mineral soil

In the mineral soil, liming had a variable response on SOC stocks. While liming may not have induced an overall significant change in SOC stocks at any soil depth (Figure 3b), the direction and magnitude of net SOC changes in response to liming at each site hinged on the strength of different processes at each site. These are primarily influenced by the sites' biochemical conditions and forest type. The observed variable response is driven by the dynamic balance in soil carbon accumulation rates, namely organic matter inputs, its stabilization and losses as CO₂ or dissolved organic carbon (Jackson et al., 2017). Considering the broad biophysical spectrum of sites we sampled at, this net C balance (losses versus gains) varied considerably in response to the increases in soil pH and base saturation in the topsoil. Like in the forest floor layer, SOC losses can be attributed to the stimulation of microbial decomposition of organic matter. The direction and magnitude of the liming-induced SOC stock changes in the mineral soil (at all soil sampling depths) could however best be explained by the soil's SOC storage capacity and how much carbon was stored therein. Generally, we found that sites with low inherent soil carbon contents (in the control plots) exhibited SOC increases, while at the other end of the spectrum those sites with inherently high carbon contents, exhibited decreases in SOC (Figure 5). This trend was also observed by van Straaten et al. (2015) after land-use change, and shows that sites with inherently high SOC stocks are more vulnerable to SOC losses than sites which initially had little to lose. When we separated our dataset into "carbon rich" (SOC content > 5.5 % at 0-5 cm depth) and "carbon poor" sites (SOC content < 5.5 %) we recorded significant increases in SOC stocks in those sites which initially had low carbon (Figure 3c), but no significant change for sites with initially high SOC stocks. The lack of a significant response in this case likely reflects that we did not sample many sites with inherently high soil carbon. Considering the "carbon-poor" sites mostly had low clay contents (high sand and low clay), and low soil fertility, the corresponding SOC increases after liming likely reflect a re-equilibration of the ecosystem carbon cycling dynamics (Figure 3d). We suspect, that C stocks were initially depleted at these sites because sustained acidification over decades which will likely have constrained aboveground net primary productivity, and accordingly reduced C inputs into the soil. Subsequent improvements in nutrient availability and reduced Al toxicity as a result of liming likely improved tree growth (Court et al., 2018, Van der Perre et al., 2012), which in turn increased C inputs into the soil. These suppositions are supported by Grüneberg et al., (2019), who similarly report that liming led to high C accumulations at sites with low clay contents, and C losses at sites with high clay contents.



454 Next, improvements in both the biochemical environment and litter palatability will likely have
stimulated earthworm bioturbation (Persson et al., 2021), especially considering earthworm
456 abundance is positively related to calcium availability (Hobbie et al., 2006, Reich et al., 2005). And while
earthworm activity is known to promote organic matter mineralization (Lubbers et al., 2017), they also
458 foster the stabilization of physico-chemically protected carbon in soil aggregates by building up
mineral-protected microbial necromass (Angst et al., 2019). It is also suspected that the decreases in
460 soil bulk densities in the topsoil (Figure A2b) are attributed to this intensified earthworm activity in the
liming plots, which will have loosened and aerated the soil improving gas diffusion, therein also
462 incorporating SOM from the O_h into the mineral soil. Although the net effect of earthworm activity on
SOC stocks may not be clear (Persson et al., 2021), it may offer an insight into why net SOC stocks
464 significantly increased in the topsoil (0-5 cm) in the broadleaf forest sites (Figure 3a) where leaf Ca
increased as a result of liming, but not in the coniferous forests where needle Ca did not improve (data
466 not shown). Another possible mechanism for the measured increases is through Ca-SOM bridging.
Here, the divalent Ca^{2+} cations bonded on negatively charged organic matter exchange complexes
468 which stabilize the SOM, thereby reducing the dissolution and mobility of the SOM (Kalbitz et al., 2000)
and correspondingly also reducing decomposition processes (Grüneberg et al., 2019; Melvin et al.,
470 2013).

4.3 Liming effects on soil respiration and soil methane fluxes

472 The comparable soil respiration rates measured in the limed and control plots at the DAS 4227 site
prior to a third lime application, highlight that (at least at this site) soil organic matter mineralization
474 rates had equilibrated after liming (done 27 years prior, Figure 6a-c). The third application of lime (in
August 2020) consequently elicited a pronounced and prolonged increase in soil respiration rates at
476 all three sites (Rosikova et al., 2019). These increases were primarily driven by biotic sources with only
a very minor contribution (<3 %) coming from lime-derived CO_2 (Figure 6a-c). This is in agreement with
478 Biasi et al. (2008) who measured similarly low abiotic CO_2 production in a limed peatland forest in
Finland. It is most likely that the resulting improvements in the soil biochemical environment created
480 suitable conditions for microbial populations to mineralize organic complexes, which led to the
increased CO_2 production. However, like SOC stock responses to lime application, the size (and
482 duration) of the CO_2 production increase varied for the three sites. Notably, the two sites with thick
SOM horizons (SEL 34 and GOH 157) had smaller and also shorter-lived CO_2 flushes than the more
484 fertile site (DAS 4227). This again supports the earlier observations that especially at poorer sites
characterized with thick forest floor layers, liming responses may be inhibited by the adsorption of
486 lime to SOM complexes.



Interestingly, long-term soil CH₄ uptake in the limed plots was more than twice that of the control plot at the Dassel 4227 site (Figure 6b). Although, we did not take baseline measurements at the other two sites, they too had double the CH₄ consumption than their respective control plots after liming. This strong CH₄ consumption corresponds to the findings of Borken and Brumme (1997), who attributed this to the fact that liming improves both the soil structure (Bronick and Lal, 2005, Schack-Kirchner and Hildebrand, 1998) and reduces the forest floor layer thickness, which in turn improves CH₄ diffusion into the soil. Furthermore, it has been shown that methanotroph abundance and activity is optimal at pHs just below 6 (Amaral et al., 1998). Despite these soils being a relatively large CH₄ sink, their CO₂ equivalency (global warming potential) nevertheless is still dwarfed by CO₂ emissions from organic matter mineralization.

5. Conclusions

We hypothesized that liming would lead to decreases in the forest floor layer C stock and that these C losses would be offset, if not exceeded, by significant gains in SOC stocks in the topsoil. Liming indeed resulted in significant decreases in forest floor SOC stocks, but these losses were only partially offset by small gains made in the mineral soil under certain conditions. However, the question of whether liming enhances forest soil C sequestration is not straight forward. Although there were overall decreases in C stocks in the forest floor, the size of these losses depended on the inherent pH and decomposability of the organic material (before liming). While liming stimulated decomposition at most sites, some poorer quality sites which were characterized by thick organic matter accumulations exhibited either only minor C losses, and in a few plots even C gains. Although there were no significant changes in SOC stocks in the mineral soil as a result of liming, the direction and magnitude of C stock changes here were likewise site-dependent. Specifically, sites with sandy soils and/or inherently low C storage exhibited large increases in SOC stocks as a result of liming, while on the other hand, C rich sites were more predisposed to C losses, suggesting that the SOC stocks here were more vulnerable to decomposition than at sites which had little to lose.

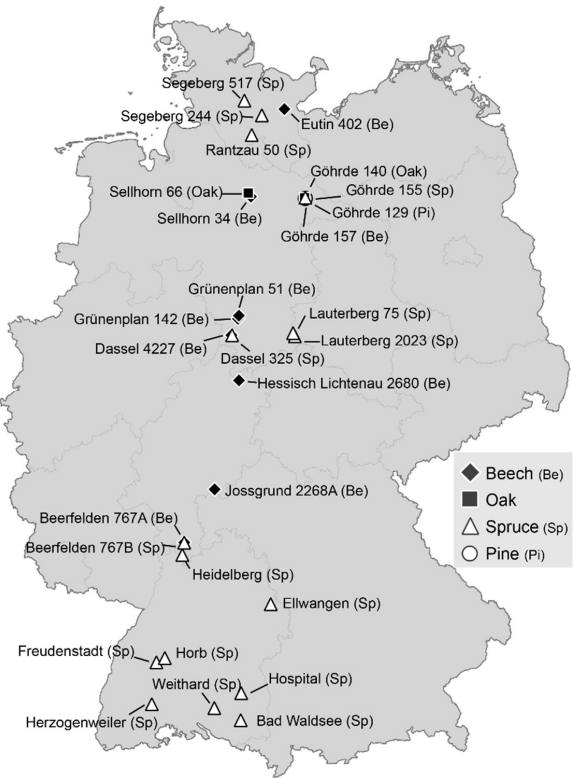
Independent of liming, there is evidence of C accumulation in the forest floor layers over the last few decades (likely a response to elevated N deposition), but liming was able to moderate the amount of C that has become immobilized in the organic matter. Liming-induced increases in mineralization rates seem to last for only a limited amount of time, as seen on the respiration rates of the soil, while the doubling in methane consumption due to liming lasts for several decades. Still, CO₂-emissions dwarf the CH₄-consumption of the soil.



We can conclude that liming has an influence on forest soil organic carbon stocks. The effect is largest
520 in the forest floor, where liming counteracts the observed temporal organic matter accumulation (due
to N deposition), thereby reducing nutrient immobilization in the forest floor. In the mineral soil the
522 effect of liming on soil organic carbon stocks is less pronounced, but there are indications that liming
promotes some carbon accumulation processes in the topsoil. In total, the implications of liming on
524 forest soil greenhouse gas budgets are small, but highly site-specific.



526 **Appendix A**
Supplement

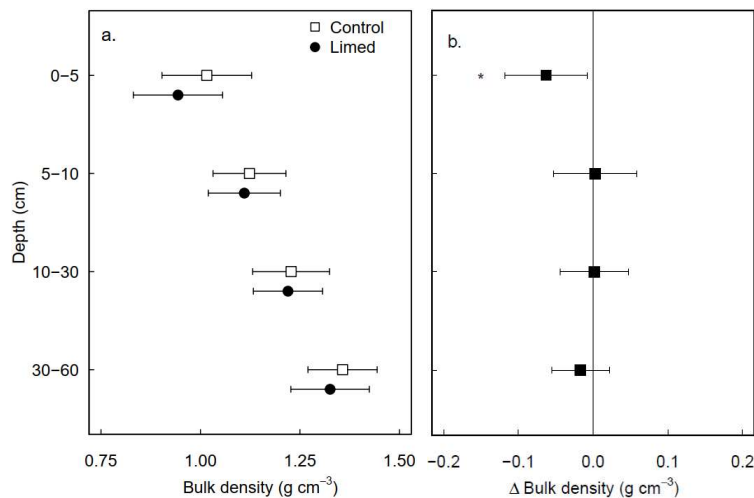


528

530 **Figure A1:** Location of the 28 paired liming experiment sites in Germany where soil organic carbon
531 samples were collected.

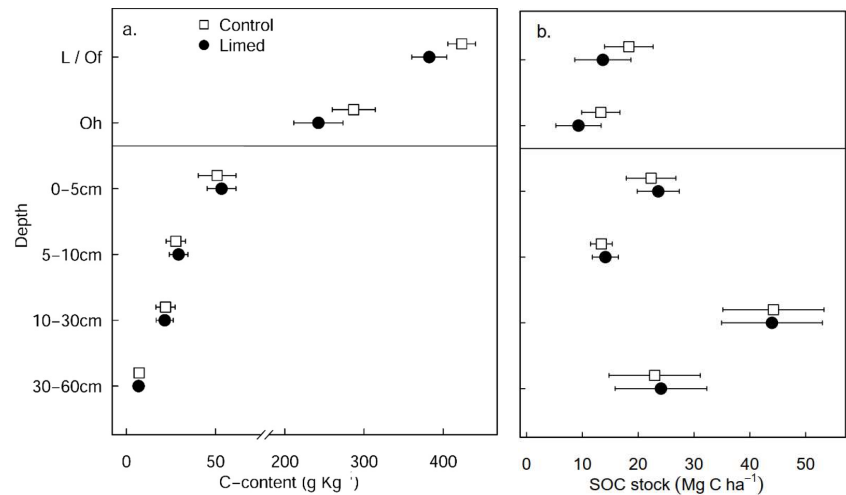
532 **Table A1:** Years when forest floor and mineral soil samples were collected from the different sites

| Site name | Species | Forest floor | Mineral soil |
|----------------------|---------|------------------------------|------------------------|
| Dassel 325 | Spruce | 1990, 1998, 2004, 2011, 2015 | 1998, 2011, 2015 |
| Dassel 4227 | Beech | 1998, 2004, 2012, 2015, 2018 | 1998, 2012, 2018 |
| Eutin 402 | Spruce | 1990, 1998, 2010 | 1998, 2010, |
| Gohrde 129 | Spruce | 1990, 1998, 2010, 2015 | 1990, 1998, 2010, 2015 |
| Gohrde 140 | Oak | 1990, 1998, 2010, 2015 | 1990, 1998, 2010, 2015 |
| Gohrde 155 | Spruce | 1990, 1998, 2013 | - |
| Gohrde 157 | Beech | 1990, 1998, 2015, 2018 | 1990, 1998, 2018 |
| Grunenplan 142 | Beech | 1990, 1998, 2009, 2015, 2018 | 1998, 2009, 2018 |
| Grunenplan 51 | Beech | 1990, 2019 | - |
| Hess. Lichtenau 2680 | Beech | - | 2012, 2018 |
| Lauterberg 2023 | Spruce | 2000, 2009, 2015 | - |
| Lauterberg 75 | Spruce | - | 1998, 2005, 2015 |
| Rantza 50 | Spruce | 2000, 2010, 2017 | 2000, 2010, 2017 |
| Segeberg 244 | Spruce | 1990, 1998, 2004, 2017 | - |
| Segeberg 517 | Spruce | 2000, 2010, 2017 | 2000, 2010, 2017 |
| Sellhorn 34 | Beech | 1990, 1998, 2010, 2015, 2018 | 1998, 2010, 2018 |
| Sellhorn 66 | Beech | 1990, 1998, 2010, 2015 | 1998, 2010, 2015 |



534 **Figure A2:** (a) Mean soil bulk density in the control plots of conifer and broadleaf forest plots and (b)
536 differences in soil bulk density between limed and control plots. Error bars indicate the 95 %
confidence intervals based on Student's T distribution. Statistical significance was tested using LME
models for each respective soil depth / layer at $P \leq 0.05$ (*) and $P \leq 0.01$ (**).

538



540 **Figure A3:** (a) Mean SOC contents in the limed and control plots and (b) mean SOC stocks in the limed
542 and control plots (forest floor layer n=28, mineral soil n=26). Error bars indicate the 95 % confidence
intervals based on Student's T distribution.



Table A2: Spearman correlation coefficients of SOC stock in the control plots at different soil depths with explanatory variables (forest floor layer n = 28, mineral soil n = 26).

| | L/O _f | O _h | 0-5 cm | 5-10 cm | 10-30 cm | 30-60 cm |
|---------------------------------------|------------------|----------------|---------------|---------------|---------------|----------------|
| Precipitation (mm a ⁻¹) | -0.10 | -0.21 | 0.11 | 0.07 | 0.14 | 0.29 |
| Temperature (°C) | -0.26 | -0.06 | -0.16 | -0.24 | -0.37 | -0.31 |
| Elevation (m.asl) | -0.23 | -0.26 | -0.10 | -0.06 | 0.32 | 0.13 |
| N-deposition (kg N ha ⁻¹) | 0.41* | 0.31 | 0.30 | 0.38 | 0.13 | 0.26 |
| Clay (%) | - | - | 0.49 | 0.51 | 0.62* | 0.23 |
| Sand (%) | - | - | -0.62* | -0.56* | -0.43 | -0.35 |
| C:N ratio | -0.01 | 0.65** | -0.05 | 0.11 | 0.13 | 0.32 |
| Base saturation (%) | 0.07 | 0.07 | -0.07 | -0.33 | -0.38 | -0.48* |
| pH (H ₂ O) | -0.79** | -0.67** | -0.27 | -0.29 | -0.41* | -0.63** |

* Indicates a P-value of ≤0.05, and ** indicates a P-value of <0.01

Table A3: Spearman correlation coefficients of SOC stock changes (limed minus control) at different soil depths with explanatory variables (forest floor layer n = 28, mineral soil n = 26).

| | L/O _f | O _h | 0-5 cm | 5-10 cm | 10-30 cm | 30-60 cm |
|---|------------------|----------------|-----------------|----------------|----------------|---------------|
| Climate and site characteristics | | | | | | |
| Precipitation (mm a ⁻¹) | 0.29 | 0.13 | 0.08 | -0.23 | 0.01 | -0.25 |
| Temperature (°C) | 0.06 | -0.28 | 0.12 | 0.09 | 0.19 | -0.09 |
| Elevation (m. asl) | 0.05 | -0.10 | 0.00 | -0.27 | -0.08 | -0.12 |
| Acid neutralization capacity (kmolc ha ⁻¹) | -0.44 * | -0.46 * | -0.08 | -0.34 § | 0.08 | 0.01 |
| Nitrogen deposition (kg N ha ⁻¹) | 0.04 | 0.29 | -0.34 § | 0.02 | -0.40 * | -0.17 |
| Soil properties of the control plot | | | | | | |
| Clay (%) † | - | - | -0.53 * | 0.00 | -0.31 | -0.16 |
| Sand (%) † | - | - | 0.43 | 0.13 | 0.50 § | 0.04 |
| SOC stock (Mg C ha ⁻¹) | -0.38 * | -0.06 | -0.55 ** | -0.32 | -0.28 | -0.28 |
| C:N ratio | -0.00 | 0.03 | 0.15 | 0.34 § | 0.14 | 0.02 |
| Base saturation (%) ‡ | 0.11 | 0.04 | -0.27 | -0.08 | 0.00 | 0.15 |
| pH (H ₂ O) | 0.14 | -0.16 | -0.12 | 0.11 | -0.17 | 0.11 |
| Changes in soil properties as a result of liming | | | | | | |
| Δ H ⁺ | 0.27 | 0.06 | 0.04 | 0.47 * | 0.26 | 0.49 * |
| Δ Base saturation ‡ | -0.23 | -0.40 | 0.11 | -0.33 § | -0.12 | -0.26 |

Levels of significance: § p < 0.10, * P ≤ 0.05, ** P ≤ 0.01, † n=15, ‡ n=11 in the forest floor layers

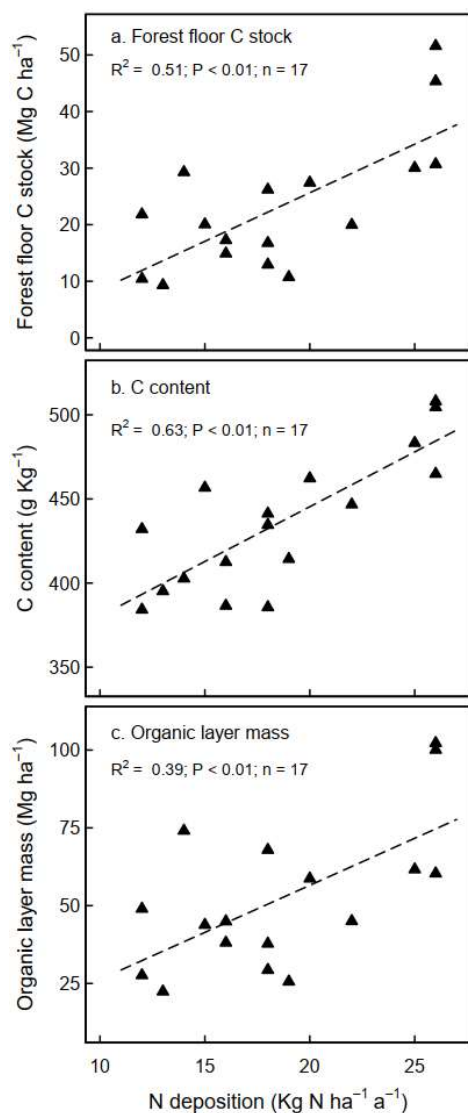
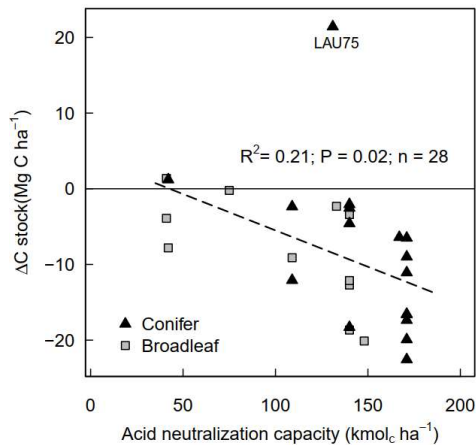
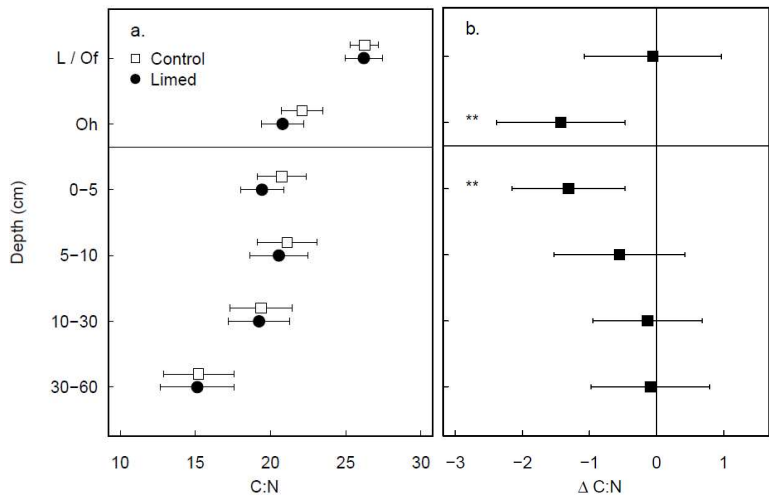


Figure A4: Effects of N deposition on (a) SOC stock (b) C content and (c) dry mass of the L/O_f horizon in unlimed coniferous forests. There was no significant correlation evident with broadleaf forests sites.



556

558 **Figure A5:** Changes in forest floor C stock (L/O_f and O_h) between limed and control plots in relation to liming quantities, expressed as acid neutralization capacity (ANC). LAU 75 is Lauterberg 75.



560

562 **Figure A6:** (a) Mean C:N ratio of limed and control plots and (b) treatment difference at different
564 depths in the 60 cm soil profile. Error bars indicate the 95 % confidence intervals based on Student's T
models for each respective soil depth / layer at $P \leq 0.05$ (*) and $P \leq 0.01$ (**).

566



Author contributions

568 The project was conceptualized UT and DZ. UT, DZ, LK coordinated the data collection activities and
oversaw the maintenance of the liming pairs. GM calculated the lime-derived CO₂ emissions. OvS did
570 the data analysis and prepared the paper. UT, DZ, LK and GM gave critical feedback on the paper.

572 Competing interests

The authors declare that they have no conflict of interest.

574

Acknowledgements

576 This study was financed by the Agency for Renewable Resources (Fachagentur Nachwachsende
Rohstoffe e.V.) under the grant 28W-B-4-075-01. The authors gratefully acknowledge Dr. Peter
578 Hartmann, Lelde Jansone and the Forest Research Institute Baden-Wuerttemberg for the soil
biochemical data from eight liming experiment sites. We also kindly acknowledge Dr. Karl Josef Meiwes
580 and Dr. Jan Evers for valuable input in the data analysis and interpretation. We also thank Lena
Wunderlich for her assistance collecting the soil GHG samples.

582



References

- 584 Amaral, J. A., Ren, T., and Knowles, R.: Atmospheric Methane Consumption by Forest Soils and
586 Extracted Bacteria at Different pH Values, *Applied and Environmental Microbiology*, 64, 2397–2402,
<https://doi.org/10.1128/AEM.64.7.2397-2402.1998>, 1998.
- Andersson, S. and Nilsson, S. I.: Influence of pH and temperature on microbial activity, substrate
588 availability of soil-solution bacteria and leaching of dissolved organic carbon in a mor humus, *Soil
Biology and Biochemistry*, 33, 1181–1191, [https://doi.org/10.1016/S0038-0717\(01\)00022-0](https://doi.org/10.1016/S0038-0717(01)00022-0), 2001.
- 590 Angst, G., Mueller, C. W., Prater, I., Angst, Š., Frouz, J., Jílková, V., Peterse, F., and Nierop, K. G. J.:
Earthworms act as biochemical reactors to convert labile plant compounds into stabilized soil
592 microbial necromass, *Communications Biology*, 2, 441, <https://doi.org/10.1038/s42003-019-0684-z>,
2019.
- 594 Biasi, C., Lind, S. E., Pekkarinen, N. M., Huttunen, J. T., Shurpali, N. J., Hyvönen, N. P., Repo, M. E., and
Martikainen, P. J.: Direct experimental evidence for the contribution of lime to CO₂ release from
596 managed peat soil, *Soil Biology and Biochemistry*, 40, 2660–2669,
<https://doi.org/10.1016/j.soilbio.2008.07.011>, 2008.
- 598 Blake, G. R. and Hartge, K. H.: Bulk Density, edited by: Klute, A., *Methods of Soil Analysis*, 363–375,
1986.
- 600 Borken, W. and Brumme, R.: Liming practice in temperate forest ecosystems and the effects on CO₂,
N₂O and CH₄ fluxes, *Soil Use and Management*, 13, 251–257, <https://doi.org/10.1111/j.1475-2743.1997.tb00596.x>, 1997.
- 602
- Bronick, C. J. and Lal, R.: Soil structure and management: a review, *Geoderma*, 124, 3–22,
604 <https://doi.org/10.1016/j.geoderma.2004.03.005>, 2005.
- Court, M., Van der Heijden, G., Didier, S., Nys, C., Richter, C., Goutal, N., Saint-Andre, L., and Legout,
606 A.: Long-term effects of forest liming on mineral soil, organic layer and foliage chemistry: Insights
from multiple beech experimental sites in Northern France, *Forest Ecology and Management*, 409,
608 872–889, <https://doi.org/10.1016/j.foreco.2017.12.007>, 2018.
- Crawley, M. J.: *The R Book*, Second edition. Chichester, West Sussex, United Kingdom : Wiley, 2013.,
610 2013.
- Derome, J.: Effects of forest liming on the nutrient status of podzolic soils in Finland, *Water, Air, and
612 Soil Pollution*, 54, 337–350, <https://doi.org/10.1007/BF00298677>, 1990.
- Derome, J., Kukkola, M., Smolander, A., and Lehto, T.: Liming of Forest Soils, in: *Forest Condition in a
614 Changing Environment: The Finnish Case*, edited by: Mälkönen, E., Springer Netherlands, Dordrecht,
328–337, https://doi.org/10.1007/978-94-015-9373-1_39, 2000.
- 616 Eklund, L. and Eliasson, L.: Effects of calcium ion concentration on cell wall synthesis, *Journal of
Experimental Botany*, 41, 863–867, <https://doi.org/10.1093/jxb/41.7.863>, 1990.
- 618 Grüneberg, E., Schöning, I., Riek, W., Ziche, D., and Evers, J.: Carbon Stocks and Carbon Stock Changes
in German Forest Soils, in: *Status and Dynamics of Forests in Germany*, vol. 237, edited by:
620 Wellbrock, N. and Bolte, A., Springer International Publishing, Cham, 167–198,
https://doi.org/10.1007/978-3-030-15734-0_6, 2019.



- 622 Hobbie, S. E., Reich, P. B., Oleksyn, J., Ogdahl, M., Zytowski, R., Hale, C., and Karolewski, P.: Tree
Species Effects on Decomposition and Forest Floor Dynamics in a Common Garden, *Ecology*, 87,
624 2288–2297, [https://doi.org/10.1890/0012-9658\(2006\)87\[2288:TSEODA\]2.0.CO;2](https://doi.org/10.1890/0012-9658(2006)87[2288:TSEODA]2.0.CO;2), 2006.
- Jackson, R. B., Lajtha, K., Crow, S. E., Hugelius, G., Kramer, M. G., and Piñeiro, G.: The Ecology of Soil
626 Carbon: Pools, Vulnerabilities, and Biotic and Abiotic Controls, *Annu. Rev. Ecol. Evol. Syst.*, 48, 419–
445, <https://doi.org/10.1146/annurev-ecolsys-112414-054234>, 2017.
- 628 Jansone, L., von Wilpert, K., and Hartmann, P.: Natural Recovery and Liming Effects in Acidified Forest
Soils in SW-Germany, *Soil Syst.*, 4, 38, <https://doi.org/10.3390/soilsystems4030038>, 2020.
- 630 Kalbitz, K., Solinger, S., Park, J.-H., Michalzik, B., and Matzner, E.: Controls on the Dynamics of
Dissolved Organic Matter in Soils: A Review, *Soil Science*, 165, 277–304,
632 <https://doi.org/10.1097/00010694-200004000-00001>, 2000.
- Knorr, M., Frey, S. D., and Curtis, P. S.: Nitrogen addition and litter decomposition: a meta-analysis,
634 *Ecology*, 86, 3252–3257, <https://doi.org/10.1890/05-0150>, 2005.
- König, N., Blum, U., Symosse, F., Bussian, B., Furtmann, K., Gärtner, A., Groetcke, K., Gutwasser, F.,
636 Höhle, J., Hauenstein, M., Kiesling, G., Klingenberg, U., Klinger, T., Nack, T., Stahn, M., Trefz-Malcher,
G., and Wies, K.: *Handbuch Forstliche Analytik: Eine Loseblatt-Sammlung der Analysemethoden im*
638 *Forstbereich*, Bundesministerium für Verbraucherschutz, Ernährung und Landwirtschaft., Bonn, 678
pp., 2014.
- 640 Kreutzer, K.: Effects of forest liming on soil processes, *Plant and Soil*, 168, 447–470,
<https://doi.org/10.1007/BF00029358>, 1995.
- 642 Lin, N., Bartsch, N., Heinrichs, S., and Vor, T.: Long-term effects of canopy opening and liming on leaf
litter production, and on leaf litter and fine-root decomposition in a European beech (*Fagus sylvatica*
644 L.) forest, *Forest Ecology and Management*, 338, 183–190,
<https://doi.org/10.1016/j.foreco.2014.11.029>, 2015.
- 646 Long, R. P., Bailey, S. W., Horsley, S. B., Hall, T. J., Swistock, B. R., and DeWalle, D. R.: Long-Term
Effects of Forest Liming on Soil, Soil Leachate, and Foliage Chemistry in Northern Pennsylvania, *Soil*
648 *Science Society of America Journal*, 79, 1223–1236, <https://doi.org/10.2136/sssaj2014.11.0465>,
2015.
- 650 Lubbers, I. M., Pulleman, M. M., and Van Groenigen, J. W.: Can earthworms simultaneously enhance
decomposition and stabilization of plant residue carbon?, *Soil Biology and Biochemistry*, 105, 12–24,
652 <https://doi.org/10.1016/j.soilbio.2016.11.008>, 2017.
- Lundström, U. S., Bain, D. C., Taylor, A. F. S., and van Hees, P. A. W.: Effects of Acidification and its
654 Mitigation with Lime and Wood Ash on Forest Soil Processes: A Review, *Water, Air and Soil Pollution:*
Focus, 3, 5–28, <https://doi.org/10.1023/A:1024115111377>, 2003.
- 656 Marschner, B. and Wilczynski, W. A.: The effect of liming on quantity and chemical composition of
soil organic matter in a pine forest in Berlin, Germany, *Plant and Soil*, 137, 229–236,
658 <https://doi.org/10.1007/BF00011201>, 1991.
- Martinson, G. O., Pommerenke, B., Brandt, F. B., Homeier, J., Burneo, J. I., and Conrad, R.:
660 Hydrogenotrophic methanogenesis is the dominant methanogenic pathway in neotropical tank
bromeliad wetlands., *Environ Microbiol Rep*, 10, 33–39, <https://doi.org/10.1111/1758-2229.12602>,
662 2018.



- 664 Melvin, A. M., Lichstein, J. W., and Goodale, C. L.: Forest liming increases forest floor carbon and
nitrogen stocks in a mixed hardwood forest, *Ecological Applications*, 23, 1962–1975,
<https://doi.org/10.1890/13-0274.1>, 2013.
- 666 Moore, T. R., Trofymow, J. A., Prescott, C. E., Titus, B. D., and CIDET Working Group: Nature and
nurture in the dynamics of C, N and P during litter decomposition in Canadian forests, *Plant and Soil*,
668 339, 163–175, <https://doi.org/10.1007/s11104-010-0563-3>, 2011.
- Persson, H. and Ahlström, K.: The effects of forest liming on fertilization on fine-root growth, *Water,
670 Air, and Soil Pollution*, 54, 365–375, <https://doi.org/10.1007/BF02385231>, 1990.
- Persson, T., Andersson, S., Bergholm, J., Grönqvist, T., Högbom, L., Vegerfors, B., and Wirén, A.: Long-
672 Term Impact of Liming on Soil C and N in a Fertile Spruce Forest Ecosystem, *Ecosystems*, 24, 968–987,
<https://doi.org/10.1007/s10021-020-00563-y>, 2021.
- 674 R Core Team: R: A language and environment for statistical computing, R Foundation for Statistical
Computing, Vienna, Austria, 2020.
- 676 Reich, P. B., Oleksyn, J., Modrzyński, J., Mrozinski, P., Hobbie, S. E., Eissenstat, D. M., Chorover, J.,
Chadwick, O. A., Hale, C. M., and Tjoelker, M. G.: Linking litter calcium, earthworms and soil
678 properties: a common garden test with 14 tree species, *Ecology Letters*, 8, 811–818,
<https://doi.org/10.1111/j.1461-0248.2005.00779.x>, 2005.
- 680 Rosikova, J., Darenova, E., Kucera, A., Volarik, D., and Vranova, V.: Effect of different dolomitic
limestone dosages on soil respiration in a mid-altitudinal Norway spruce stand, *iForest -
682 Biogeosciences and Forestry*, 12, 357–365, <https://doi.org/10.3832/for2894-012>, 2019.
- Schack-Kirchner, H. and Hildebrand, E. E.: Changes in soil structure and aeration due to liming and
684 acid irrigation, *Plant and Soil*, 199, 167–176, <https://doi.org/10.1023/A:1004290226402>, 1998.
- Shen, Y., Tian, D., Hou, J., Wang, J., Zhang, R., Li, Z., Chen, X., Wei, X., Zhang, X., He, Y., and Niu, S.:
686 Forest soil acidification consistently reduces litter decomposition irrespective of nutrient availability
and litter type, *Functional Ecology*, 35, 2753–2762, <https://doi.org/10.1111/1365-2435.13925>, 2021.
- 688 Siepel, H., Bobbink, R., van de Riet, B. P., van den Burg, A. B., and Jongejans, E.: Long-term effects of
liming on soil physico-chemical properties and micro-arthropod communities in Scotch pine forest,
690 *Biology and Fertility of Soils*, 55, 675–683, <https://doi.org/10.1007/s00374-019-01378-3>, 2019.
- Smolander, A., Kitunen, V., Paavolainen, L., and Mälikönen, E.: Decomposition of Norway spruce and
692 Scots pine needles: Effects of liming, *Plant and Soil*, 179, 1–7, <https://doi.org/10.1007/BF00011636>,
1996.
- 694 van Straaten, O., Corre, M. D., Wolf, K., Tchienkoua, M., Cuellar, E., Matthews, R. B., and Veldkamp,
E.: Conversion of lowland tropical forests to tree cash crop plantations loses up to one-half of stored
696 soil organic carbon, *Proc Natl Acad Sci USA*, 112, 9956–9960,
<https://doi.org/10.1073/pnas.1504628112>, 2015.
- 698 UBA: Nationale Trendtabellen für die deutsche Berichterstattung atmosphärischer Emissionen,
Umweltbundesamt, Dessau, 2019.
- 700 Van der Perre, R., Jonard, M., André, F., Nys, C., Legout, A., and Ponette, Q.: Liming effect on radial
growth depends on time since application and on climate in Norway spruce stands, *Forest Ecology
702 and Management*, 281, 59–67, <https://doi.org/10.1016/j.foreco.2012.06.039>, 2012.



- 704 Wendt, J. W. and Hauser, S.: An equivalent soil mass procedure for monitoring soil organic carbon in
multiple soil layers, *European Journal of Soil Science*, 64, 58–65, <https://doi.org/10.1111/ejss.12002>,
2013.
- 706 Xing, K., Zhao, M., Niinemets, Ü., Niu, S., Tian, J., Jiang, Y., Chen, H. Y. H., White, P. J., Guo, D., and
Ma, Z.: Relationships Between Leaf Carbon and Macronutrients Across Woody Species and Forest
708 Ecosystems Highlight How Carbon Is Allocated to Leaf Structural Function, *Frontiers in Plant Science*,
12, 1030, <https://doi.org/10.3389/fpls.2021.674932>, 2021.

710